Chem. Res. Toxicol. **2004,** *17,* 1750−1756

Oxidative DNA Damage Induced by Carcinogenic Dinitropyrenes in the Presence of P450 Reductase

Mariko Murata,[†] Shiho Ohnishi,[†] Kazuharu Seike,[†] Kiyoshi Fukuhara,[‡] Naoki Miyata,[§] and Shosuke Kawanishi*,[†]

Department of Environmental and Molecular Medicine, Mie University School of Medicine, 2-174, Edobashi, Tsu, Mie 514-8507, Japan, National Institute of Health Science, 1-18-1, Kamiyouga Setagaya-ku, Tokyo 158-8501, Japan, and Department of Graduate School of Pharmaceutical Sciences, Nagoya City University, 3-1 Tanabe-dori, Mizuho-ku, Nagoya, Aichi 467-8603, Japan

Received September 2, 2004

Nitropyrenes are widespread in the environment due to mainly diesel engine emissions. Dinitropyrenes (DNPs), especially 1,8-dinitropyrene (1,8-DNP) and 1,6-dinitropyrene (1,6-DNP), are much more potent mutagens than other nitropyrenes. The carcinogenicity of 1,8-DNP and 1,6-DNP is stronger than 1,3-dinitropyrene (1,3-DNP). It is considered that adduct formation after metabolic activation plays an important role in the expression of carcinogenicity of nitropyrenes. However, Djuric et al. [(1993) *Cancer Lett.*] reported that oxidative DNA damage was also found as well as adduct formation in rats treated with 1,6-DNP. We investigated oxidative DNA damage by DNPs in the presence of NAD(P)H-cytochrome P450 reductase using ^{32}P-5′-end-labeled DNA. After P450 reductase treatment, DNPs induced Cu(II)-mediated DNA damage in the presence of NAD(P)H. The intensity of DNA damage by 1,8-DNP or 1,6-DNP was stronger than 1,3-DNP. We also examined synthetic 1-nitro-8-nitrosopyrene (1,8-NNOP) and 1-nitro-6-nitrosopyrene (1,6-NNOP) as one of the metabolites of 1,8-DNP and 1,6-DNP, respectively, to find that 1,8-NNOP and 1,6-NNOP induced Cu(II)-mediated DNA damage in the presence of NAD(P)H but untreated DNPs did not. In both cases of P450 reductase-treated DNPs and NNOPs, catalase and a Cu(I) specific chelator attenuated DNA damage, indicating the involvement of H_2O_2 and Cu(I). Using a Clarke oxygen electrode, oxygen consumption by the reaction of NNOPs with NAD(P)H and Cu(II) was measured to find that NNOP was nonenzymatically reduced by NAD(P)H and that the addition of Cu(II) promoted the redox cycle. Therefore, these results suggest that DNPs are enzymatically reduced to NNOPs via nitro radical anion and that NNOPs are further reduced nonenzymatically by NAD(P)H. Subsequently, autoxidation of nitro radical anion and the reduced form of NNOP occurs, resulting in O_2^- generation and DNA damage. We conclude that oxidative DNA damage in addition to DNA adduct formation may play important roles in the carcinogenesis of DNPs via their metabolites.

Introduction

Nitropolycyclic aromatic hydrocarbons including nitropyrenes (NPs) are widespread in the environment due to mainly diesel engine emissions (*1*, *2*). NPs are strongly mutagenic in the bacterial mutation assay (Ames test) and human cell mutagenicity assay (*3*, *4*). Dinitropyrenes (DNPs),[1] especially 1,8-dinitropyrene (1,8-DNP) and 1,6-dinitropyrene (1,6-DNP), are much more potent mutagens than other nitropyrenes. DNPs induced lung cancer and leukemia in rodents. An epidemiological study demonstrated that significant positive trends in lung cancer risk were observed with increasing cumulative exposure of diesel exhaust in male truck drivers (*5*). The International Agency for Research on Cancer (IARC) has assessed that 1,8-DNP and 1,6-DNP have been possibly carcinogenic to humans (group 2B), whereas 1,3-dinitropyrene (1,3-DNP) has not been classifiable as to its carcinogenicity to humans (group 3) (*1*).

Chemical mutagenesis is strongly affected by metabolic activation. Cellular nitroreductase and *O*-acetyltransferase activities have been shown to markedly influence the genotoxic activity of nitro-aromatic compounds (*6*). DNA adduct formation after metabolic activation has been considered to be a major causal factor of carcinogenesis by DNPs. DNPs undergo nitroreduction to *N*-hydroxy arylamines that bind to DNA directly or after *O*-esterification (*1*). DNP adducts are identified as *N*-(deoxyguanosin-8-yl)amino-nitropyrene (dG-C8-1,6-ANP and dG-C8-1,8-ANP), leading to mutation and carcinogenesis (*1*, *7*). On the other hand, Djuric et al. found not only DNA adducts but also oxidative DNA damage in rats

* To whom correspondence should be addressed. Tel/Fax: +81-59-231-5011. E-mail: kawanisi@doc.medic.mie-u.ac.jp.
† Mie University School of Medicine.
‡ National Institute of Health Science.
§ Nagoya City University.

[1] Abbreviations: DNPs, dinitropyrenes; 1,3-DNP, 1,3-dinitropyrene; 1,6-DNP, 1,6-dinitropyrene; 1,8-DNP, 1,8-dinitropyrene; NNOPs, nitronitrosopyrenes; 1,6-NNOP, 1-nitro-6-nitrosopyrene; 1,8-NNOP, 1-nitro-8-nitrosopyrene; 8-oxodG, 8-oxo-7,8-dihydro-2′-deoxyguanosine; NAD(P)H, β-nicotinamide adenine dinucleotide (phosphate) (reduced form); P450 reductase, NAD(P)H-cytochrome P450 reductase; O_2^-, superoxide; ECD, electrochemical detector; DTPA, diethylenetriamine-*N*,*N*,*N*′,*N*″,*N*″-pentaacetic acid; SOD, superoxide dismutase.

10.1021/tx0497550 CCC: $27.50
Published on Web 11/24/2004

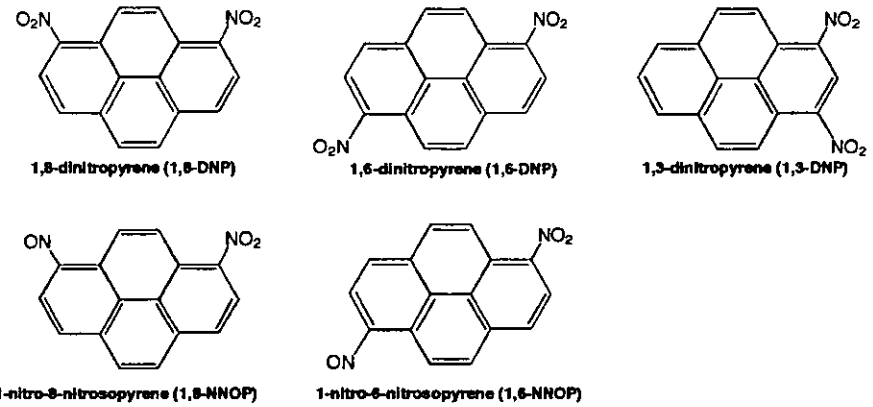

Figure 1. Chemical structures of DNPs and their metabolites used in this study.

treated with 1,6-DNP (*8*). Furthermore, we previously revealed the role of a nitroso derivative of 1-nitropyrene on causing oxidative DNA damage (*9*). It has been reported that nitro-nitroso derivatives are metabolic intermediates of DNPs during metabolic activation, which are more mutagenic than their parent DNPs (*10*). These indicate that oxidative DNA damage by DNPs after metabolic activation plays a role in carcinogenesis.

In this study, we investigated oxidative DNA damage induced by DNPs in the presence of NAD(P)H-cytochrome P450 reductase (P450 reductase), using ^{32}P-5′-end-labeled DNA fragments obtained from the human *p53* and *p16* tumor suppressor genes and the c-Ha-*ras*-1 protooncogene. We also examined synthetic nitro-nitrosopyrenes (NNOP), 1-nitro-8-nitrosopyrene (1,8-NNOP), and 1-nitro-6-nitrosopyrene (1,6-NNOP) as nitroso metabolites of DNP. The chemical structures of DNPs and synthetic NNOPs used in this study are shown in Figure 1. We also analyzed 8-oxo-7,8-dihydro-2′-deoxyguanosine (8-oxodG) formation in calf thymus DNA.

Materials and Methods

Materials. 1,6-NNOP and 1,8-NNOP were synthesized by oxidation of 1-nitro-6-aminopyrene and 1-nitro-8-aminopyrene, respectively, according to the method by the reference (*11*). The nitroaminopyrene used in the synthesis was carried out until none of the undesired isomer could be detected by ^{1}H NMR spectroscopy. To a solution of the purified aminonitropyrene dissolved in CH_3Cl, a solution of *m*-CPBA in CH_3Cl was added dropwise over 20 min and the reaction was carried out at 5 °C for 4 h. The mixture was washed with saturated $NaHCO_3$ and brine, and the organic phase was dried over anhydrous Na_2SO_4. Following evaporation in vacuo, the product was obtained by column chromatography on silica gel using *n*-hexanes−ethyl acetate as the eluent and further recrystallization from *n*-hexanes−ethyl acetate to produce light orange crystals. The purity of each compound was >99% as assessed by ^{1}H NMR spectroscopy.

1. 1,6-NNOP. ^{1}H NMR (400 MHz DMSO-d_6): δ 7.04 (1H, d, J = 8.8 Hz), 8.49 (1H, d, J = 8.8 Hz), 8.64 (1H, d, J = 9.2 Hz), 8.84 (1H, d, J = 8.4 Hz), 8.92 (1H, d, J = 8.4 Hz), 8.97 (1H, d, J = 9.6 Hz), 9.00 (1H, d, J = 9.2 Hz), 10.42 (1H, d, J = 9.6 Hz), mp 244 °C (decomp.) [lit. (*11*) >233 °C (decomp.)].

2. 1,8-NNOP. ^{1}H NMR (400 MHz DMSO-d_6): δ 7.03 (1H, d, J = 8.4 Hz), 8.49 (1H, d, J = 8.4 Hz), 8.55 (1H, d, J = 8.8 Hz), 8.71 (1H, d, J = 8.8 Hz), 8.75 (1H, d, J = 8.8 Hz), 8.92 (1H, d, J = 8.8 Hz), 9.21 (1H, d, J = 9.6 Hz), 10.45 (1H, d, J = 9.6 Hz), mp 268 °C (decomp.) [lit. (*11*) >245 °C (decomp.)].

Restriction enzymes (*Hind* III, *Sty* I, *Apa* I, *Ava* I, and *Xba* I) and T_4 polynucleotide kinase were purchased from New England Biolabs (Beverly, MA). [γ-^{32}P]ATP (222 TBq/mmol) was obtained from New England Nuclear. Alkaline phosphatase from calf intestine was purchased from Roche Molecular Biochemicals (Mannheim, Germany). 1,8-DNP, 1,6-DNP, and 1,3-DNP were purchased from Aldrich Chemical Co. (Milwaukee, IL; the purities were 98, 98, and 99%, respectively). P450 reductase from rat microsome was a kind gift from Prof. Y. Kumagai (Tsukuba University). Piperidine was purchased from Wako Chemical Industries Ltd. (Osaka, Japan). Copper(II) chloride dihydrate was purchased from Nacalai Tesque, Inc. (Kyoto, Japan). Diethylenetriamine-*N*,*N*,*N*′,*N*″,*N*″-pentaacetic acid (DTPA) and bathocuproinedisulfonic acid were purchased from Dojin Chemicals Co. (Kumamoto, Japan). Calf thymus DNA, superoxide dismutase (SOD) (3000 units/mg from bovine erythrocytes), and catalase (45000 units/mg from bovine liver) were purchased from Sigma Chemical Co. (St. Louis, MO). Nuclease P_1 (400 units/mg) was purchased from Yamasa Shoyu Co. (Chiba, Japan).

Preparation of ^{32}P-5′-End-Labeled DNA Fragments Obtained from the *p53* Gene, the *p16* Gene, and the c-Ha-*ras*-1 Gene. DNA fragments were obtained from the human *p53* and *p16* tumor suppressor gene (*12*, *13*) and the c-Ha-*ras*-1 protooncogene (*14*). A singly ^{32}P-5′-end-labeled double-stranded 443 bp fragment (*Apa* I 14179-*Eco* RI* 14621) from the *p53* gene was prepared from the pUC18 plasmid according to a method described previously (*15*). A singly labeled 328 bp fragment (*Eco*RI*5841-*Mro*I 6168) of the *p16* gene was prepared from pGEM-T Easy Vector (Promega Corporation) as described previously (*16*). A 261 bp fragment (*Ava* I* 1645-*Xba* I 1905) and a 341 bp fragment (*Xba*I 1906-*Ava*I* 2246) from the c-Ha-*ras*-1 gene were prepared from plasmid pbcNI, which carries a 6.6 kb *Bam*H I chromosomal DNA restriction fragment as described previously (*17*). The asterisk indicates ^{32}P labeling.

Detection of DNA Damage. A standard reaction mixture (in a microtube; 1.5 mL) contained $CuCl_2$, NAD(P)H, NNOP, ^{32}P-5′-end-labeled double-stranded DNA fragments, and calf thymus DNA in 200 μL of 10 mM sodium phosphate buffer (pH 7.8). For nitroreduction, DNP, 100 μM NADPH, and P450 reductase were preincubated at 25 °C for 30 min in 20 mM potassium phosphate buffer (pH 7.4). After the preincubation, ^{32}P-labeled DNA fragments, calf thymus DNA, and $CuCl_2$ were added to the mixtures (total 200 μL), followed by the incubation. After incubation at 37 °C for 1 h, DNA fragments were treated in 10% (v/v) piperidine at 90 °C for 20 min or treated with 6 units of Fpg protein in reaction buffer [10 mM HEPES−KOH (pH 7.4), 100 mM KCl, 10 mM EDTA, and 0.1 mg/mL BSA] at 37 °C for 2 h, as described previously (*18*). The treated DNA fragments were electrophoresed on an 8% polyacrylamide/8 M urea gel, and an autoradiogram was obtained by exposing X-ray film to the gel. To make the dose of DNA constant, we used calf thymus DNA (20−50 μM) at an excessive dose as compared with ^{32}P-labeled DNA (less than pM) that can be negligible, because the required dose of ^{32}P-labeled DNA, for detection of DNA damage, varies according to the decaying radioactivity (^{32}P; $T_{1/2}$ = 14 days). The preferred cleavage sites were determined by direct comparison of the positions of the oligonucleotides with those produced by the chemical reactions of the Maxam−Gilbert

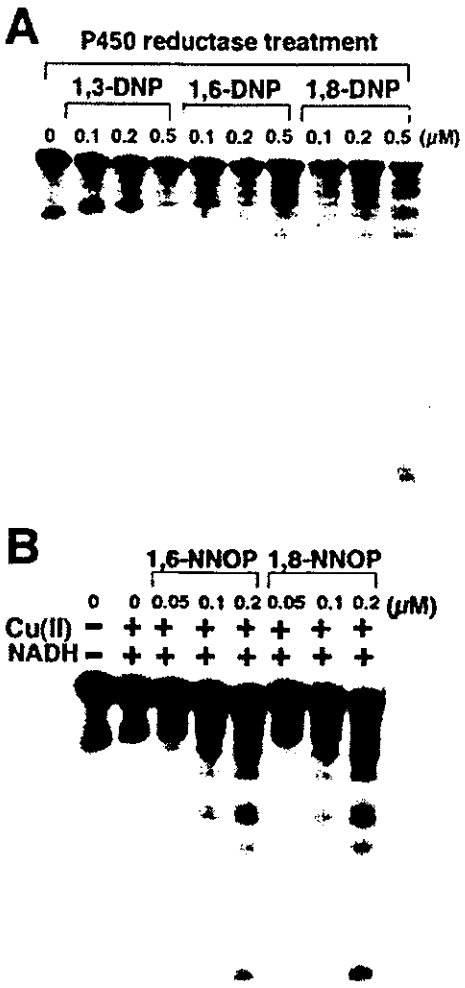

Figure 2. Autoradiogram of ^{32}P-labeled DNA fragment treated with DNPs and their nitro-nitroso derivatives. (A) The reaction mixtures containing the indicated concentrations of DNPs, 100 μM NADPH, and 2.1 μg/mL P450 reductase were preincubated at 25 °C for 30 min in potassium phosphate buffer (pH 7.4). After preincubation, a ^{32}P-5′-end-labeled 328 bp DNA fragment, calf thymus DNA (20 μM/base), and 20 μM $CuCl_2$ were added to the mixtures. (B) The reaction mixture contained a ^{32}P-5′-end-labeled 341 bp DNA fragment, calf thymus DNA (50 μM/base), the indicated concentrations of 1,8-NNOP or 1,6-NNOP, 100 μM NADH, and 20 μM $CuCl_2$ in sodium phosphate buffer (pH 7.8). The reaction mixtures were incubated at 37 °C for 1 h, followed by piperidine treatment, as described in the Materials and Methods. The DNA fragments were electrophoresed on an 8% polyacrylamide/8 M urea gel, and an autoradiogram was obtained by exposing an X-ray film to the gel.

procedure (*19*) using a DNA sequencing system (LKB 2010 Macrophor). A laser densitometer (LKB 2222 UltroScan XL) was used for the measurement of the relative amounts of oligonucleotides from the treated DNA fragments.

Analysis of 8-OxodG Formation by DNPs and NNOPs. The calf thymus DNA fragment was incubated with NNOP or treated DNP, NAD(P)H, and $CuCl_2$. After ethanol precipitation, DNA was digested to its component nucleosides with nuclease P_1 and calf intestine phosphatase and analyzed by HPLC-electrochemical detector (ECD), as described previously (*20*).

Measurement of Oxygen Consumption. Oxygen consumption by the reaction of NNOPs with NADH and $CuCl_2$ was measured using a Clarke oxygen electrode (Electronic Stirrer model 300, Rank Brothers Ltd., Bottisham Cambridge, United Kingdom). The reactions were performed in a mixture containing NNOP, NADH, and $CuCl_2$ in 2 mL of 10 mM phosphate buffer (pH 7.8) containing 2.5 μM DTPA at 37 °C. Catalase was added in order to detect H_2O_2 generation due to oxygen consumption.

Figure 3. Effects of scavengers and bathocuproine on Cu(II)/NAD(P)H-mediated DNA damage induced by P450 reductase-catalyzed 1,8-DNP and 1,8-NNOP. (A) The reaction mixtures containing 0.5 μM 1,8-DNP, 100 μM NADPH, and 2.1 μg/mL P450 reductase were preincubated at 25 °C for 30 min in potassium phosphate buffer (pH 7.4). After preincubation, a ^{32}P-5′-end-labeled 309 bp DNA fragment, calf thymus DNA (20 μM/base), 20 μM $CuCl_2$, and a scavenger were added to the mixtures. (B) The reaction mixture contained a ^{32}P-5′-end-labeled 261 bp DNA fragment, calf thymus DNA (20 μM/base), 0.2 μM 1,8-NNOP, 20 μM $CuCl_2$, and a scavenger in sodium phosphate buffer (pH 7.8). The reaction mixtures were incubated at 37 °C for 1 h, followed by piperidine treatment. The DNA fragments were analyzed as described in the legend to Figure 2. The concentrations of scavengers and bathocuproine were as follows: 0.1 M mannitol, 0.1 M sodium formate, 30 units of SOD, 30 units of catalase, and 50 μM bathocuproine.

Results

Damage to ^{32}P-Labeled DNA. Figure 2 shows an autoradiogram of a DNA fragment treated with DNPs and NNOPs. Oligonucleotides were detected on the autoradiogram as a result of DNA damage. DNPs did not cause DNA damage in the presence of NAD(P)H and Cu-

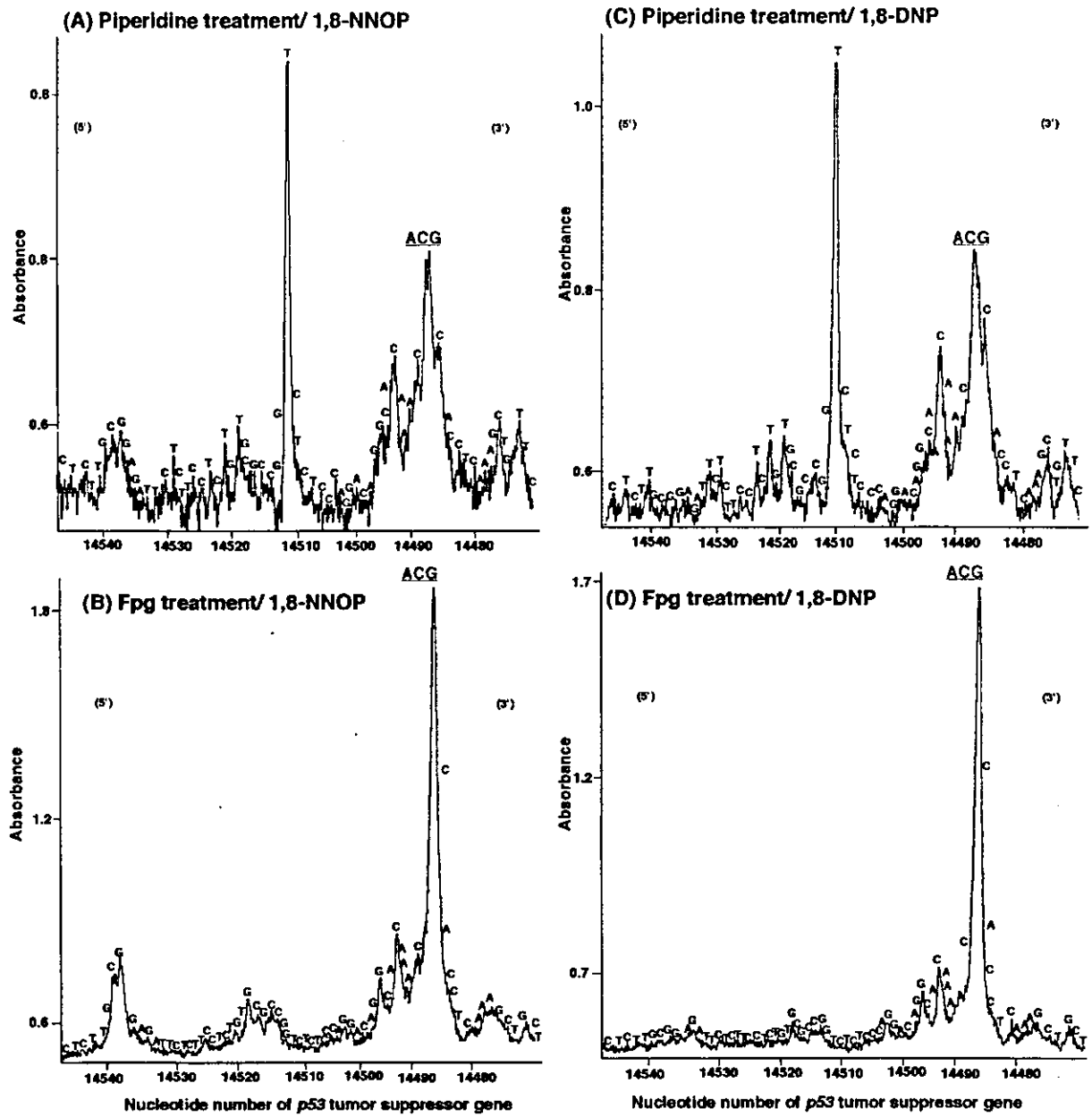

Figure 4. Site specificity of DNA cleavage induced by P450 reductase-treated 1,8-DNP and 1,8-NNOP in the presence of NADPH and Cu(II). The reaction mixtures containing 0.5 μM 1,8-NNOP (A, B) or 0.5 μM 1,8-DNP (C, D), 100 μM NADPH with (C, D) or without (A, B) 2.1 μg/mL P450 reductase were preincubated at 25 °C for 30 min in potassium phosphate buffer (pH 7.4). After preincubation, a ^{32}P-5′-end-labeled 443 bp DNA fragment, calf thymus DNA (20 μM/base), and 20 μM $CuCl_2$ were added to the mixtures. The reaction mixtures were incubated at 37 °C for 1 h, followed by piperidine treatment (A, C) or Fpg treatment (B, D). The horizontal axis shows the nucleotide number of the human *p53* tumor suppressor gene, and underscoring shows the complementary sequence to codon 273 (nucleotides 14486−14488).

(II) (data not shown). When P450 reductase was added, DNPs induced Cu(II)-mediated DNA damage (Figure 2A). 1,8-DNP and 1,6-DNP induced DNA damage more efficiently than 1,3-DNP did.

NNOPs, nitro-reduced metabolites of DNPs, were synthesized in order to compare with parent DNP. 1,8-NNOP and 1,6-NNOP induced DNA damage without P450 reductase (Figure 2B). These NNOPs induced DNA damage in the presence of NAD(P)H and Cu(II). In the absence of either NAD(P)H or Cu(II), NNOPs did not cause DNA damage. NNOPs alone did not cause DNA damage (data not shown).

Effects of Scavengers and Bathocuproine on DNA Damage. The effects of scavengers and bathocuproine on DNA damage by 1,8-DNP with P450 reductase are shown in Figure 3A. Mannitol and sodium formate, typical ·OH scavengers, did not inhibit DNA damage. Catalase and bathocuproine, a Cu(I) specific chelator, inhibited DNA damage, whereas SOD did not reduce the amount of DNA damage. Similar inhibitory effects were observed in the cases of 1,8-NNOP (Figure 3B). When 1,6-isomers were used instead of 1,8-isomers, similar results were obtained (data not shown).

Site Specificity of DNA Damage by 1,8-DNP with P450 Reductase and 1,8-NNOP. An autoradiogram was scanned with a laser densitometer to measure the relative intensities of DNA cleavage products from the human *p53* tumor suppressor gene. 1,8-NNOP and P450 reductase-treated 1,8-DNP induced piperidine labile sites relatively at thymine and cytosine residues in the pres-

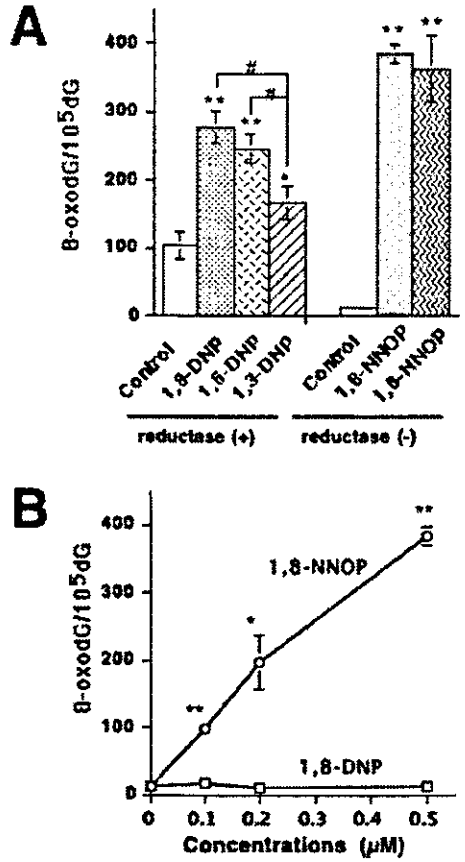

Figure 5. Formation of 8-oxodG by P450 reductase-treated DNPs and NNOPs in the presence of NADPH and Cu(II). For DNPs, the reaction mixtures containing 0.5 μM DNPs, 100 μM NADPH, and 2.1 μg/mL P450 reductase were preincubated at 25 °C for 30 min in potassium phosphate buffer (pH 7.4). After preincubation, calf thymus DNA (100 μM/base) and 20 μM $CuCl_2$ were added to the mixtures, followed by the incubation of 37 °C for 1 h. For NNOPs, the reaction mixtures containing calf thymus DNA (100 μM/base), 0.5 μM NNOPs (A), or the indicated concentrations of NNOPs (B), 100 μM NADPH, and 20 μM $CuCl_2$ were incubated at 37 °C for 1 h in potassium phosphate buffer (pH 7.4). After ethanol precipitation, DNA was enzymatically digested to individual nucleosides, and the 8-oxodG content was measured by HPLC-ECD as described in the Materials and Methods. Results are expressed as means and SD of values obtained from three independent experiments. Symbols indicate a significant difference as compared with control (*P < 0.05; **P < 0.01) and significant difference among DNPs (#P < 0.05) by t-test.

ence of Cu(II) and NAD(P)H (Figure 4A,C). With Fpg treatment, DNA cleavage occurred mainly at guanine and cytosine residues (Figure 4B,D). 1,8-NNOP and 1,8-DNP caused piperidine labile and Fpg sensitive lesions at CG in the 5′-ACG-3′ sequence, a well-known hotspot (*21*) of the *p53* gene.

Formation of 8-OxodG in Calf Thymus DNA. Using HPLC-ECD, we measured the 8-oxodG content of calf thymus DNA incubated with NNOPs and P450 reductase-treated DNPs (Figure 5A). P450 reductase-treated DNPs significantly increased the amount of 8-oxodG as compared with the control (1,8-DNP, P < 0.01; 1,6-DNP, P < 0.01; 1,3-DNP, P < 0.05). The order of 8-oxodG content was as follows: 1,8-DNP, 1,6-DNP > 1,3-DNP > control. 1,8-DNP and 1,6-DNP induced 8-oxodG formation more efficiently than 1,3-DNP (P < 0.01 and P < 0.05, respectively). There was no significant difference in 8-oxodG formation between 1,8-DNP and 1,6-DNP, after P450 reductase treatment. 1,8-NNOP and

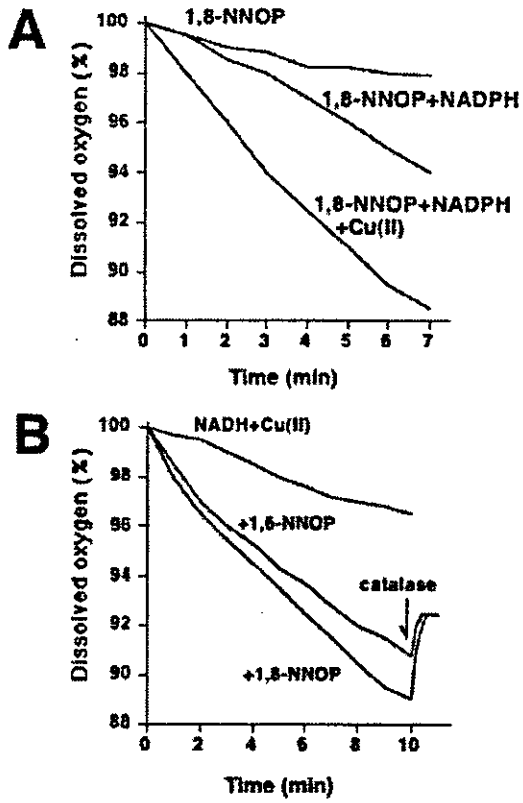

Figure 6. Oxygen consumption by the interaction of NNOPs with NAD(P)H and Cu(II). (A) Reaction mixtures contain 100 μM 1,8-NNOP, 2 mM NADPH, and/or 100 μM $CuCl_2$ in 2 mL of 10 mM phosphate buffer (pH 7.4) at 37 °C. (B) Reaction mixtures contain 100 μM NNOP, 2 mM NADH, and/or 100 μM $CuCl_2$ in 2 mL of 10 mM phosphate buffer (pH 7.8) at 37 °C. To detect H_2O_2 generation during oxygen consumption, 100 units of catalase were added at 10 min (indicated by an arrow).

1,6-NNOP without reductase significantly induced 8-oxodG formation in the presence of Cu(II) and NAD(P)H (Figure 5A).

1,8-NNOP significantly induced Cu(II)/NAD(P)H-mediated 8-oxodG formation in a dose-dependent manner (Figure 5B). 1,8-DNP induced no significant increase of 8-oxodG formation without P450 reductase. In the case of 1,6-NNOP, similar results were obtained (data not shown).

Oxygen Consumption during the Reaction of NNOP in the Presence of NADH and Cu(II). Oxygen consumption was observed in the reaction of 1,8-NNOP with NADH and Cu(II) (Figure 6). In the case of 1,8-NNOP alone, a little amount of oxygen consumption was observed. The addition of NADH increased oxygen consumption to some extent. In the reaction of 1,8-NNOP with NADH and Cu(II), a large amount of oxygen was consumed (Figure 6A). Figure 6B shows oxygen consumption by 1,8-NNOP and 1,6-NNOP in the presence of NADH and Cu(II). In the reaction of NADH and Cu(II), a little amount of oxygen consumption was observed. 1,8-NNOP induced oxygen consumption a little more efficiently than 1,6-NNOP. The addition of catalase increased dissolved oxygen, suggesting the generation of H_2O_2 that was decomposed by catalase to yield oxygen.

Discussion

The present study demonstrated the abilities of oxidative DNA damage by DNPs and their nitroso metabolites. NNOPs caused oxidative DNA damage in the presence

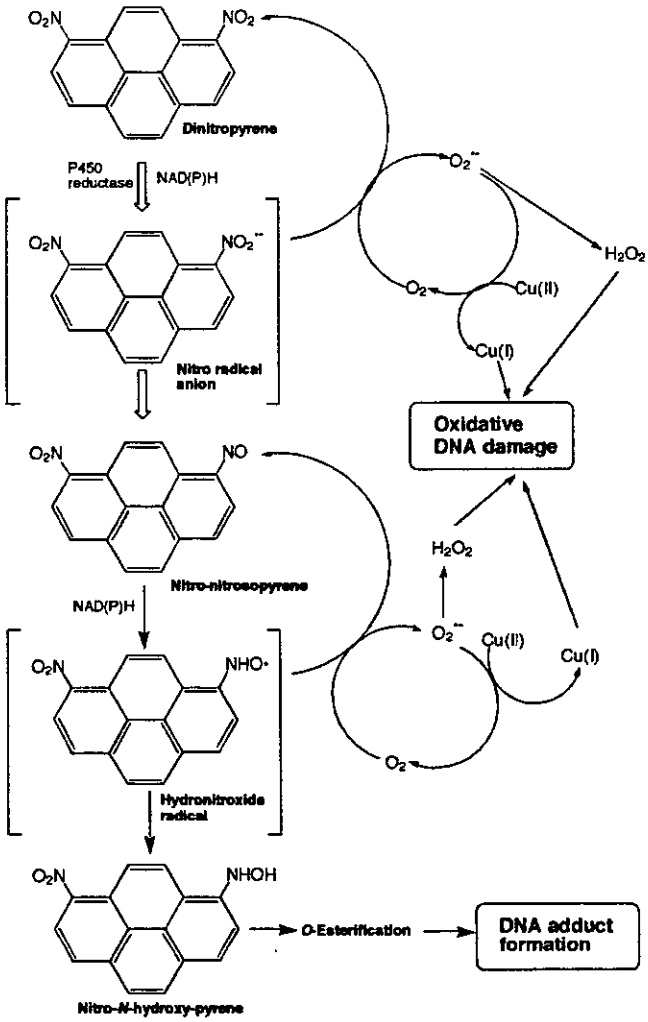

Figure 7. Proposed mechanism of oxidative DNA damage induced by DNPs in the presence of P450 reductase, NAD(P)H, and Cu(II).

of NAD(P)H and Cu(II), but DNPs did not. After the treatment of P450 reductase, DNPs, especially 1,8-DNP and 1,6-DNP, induced Cu(II)-mediated DNA damage. Both catalase and bathocuproine were found to reduce the DNA damage, indicating the involvement of H_2O_2 and Cu(I). These results suggested that NNOP was nonenzymatically reduced by NAD(P)H and autoxidized again by reacting with molecular oxygen to generate superoxide (O_2^-), and the addition of Cu(II) promoted the redox cycle. On the basis of these results, a possible mechanism could be proposed as follows (Figure 7). P450 reductase catalyzes one or more electron reduction of DNP to nitro radical anion and/or further reduced forms. Autoxidation of the reduced form yields O_2^-. NNOP can be reduced by an endogenous reductant NAD(P)H, to a reactive intermediate, which is probably a hydronitroxide radical. Autoxidation of this intermediate to NNOP occurs, coupled with the generation of O_2^-. O_2^- is dismutated to H_2O_2 and reduces Cu(II) to Cu(I). H_2O_2, in turn, interacts with Cu(I) to form a reactive oxygen species, which causes DNA damage. Study using a Clarke oxygen electrode confirmed oxygen consumption by the reaction of NNOPs with NADH and Cu(II). The addition of catalase increased the level of dissolved oxygen by the decomposition of H_2O_2 to oxygen. It is suggested that the dissolved oxygen in the reaction mixture is converted to O_2^- by the reduced forms of DNPs and NNOPs. Collectively, NNOP and P450 reductase-treated DNP significantly induce DNA damage including 8-oxodG formation through NAD(P)H-dependent redox cycles. The amounts of 8-oxodG induced by DNPs and NNOPs (0.5 μM) through the redox cycles corresponded to those induced by 30−60 μM H_2O_2 in the presence of Cu(II). The concentration of NAD(P)H in certain tissue has been estimated to be as high as 100−200 μM (*22*). The biological importance of NADH and NADPH as nuclear reductants (*23*) has been demonstrated before (*24*, *25*). P450 reductase and other enzymes with nitroreduction activity, such as NAD(P)H:quinone oxidoreductase and xanthine oxidase (*26*, *27*), may participate in activation of DNPs in vivo.

We showed that DNPs with P450 reductase treatment induced DNA damage including 8-oxodG formation in the intensity of 1,8-DNP, 1,6-DNP > 1,3-DNP. Consistently, among three DNP isomers, 1,3-DNP appears to be a weaker carcinogen (*1*) and mutagen (*3*, *4*). 1,6-DNP and 1,8-DNP are more efficiently nitro-reduced by liver cytosol and microsomes than 1,3-DNP (*28*). Similarly, Djuric (*29*) demonstrated that NADPH-mediated reduction of 1,3-NNOP to intermediates was slower than that of 1,6-NNOP. These differences in rates of enzyme efficacy to DNPs are considered to be one factor contributing to the differences of DNA damaging ability. This may explain the lower carcinogenic potential of 1,3-DNP as compared to 1,6-DNP and 1,8-DNP. Our results have suggested that DNPs are enzymatically reduced to NNOPs and are subsequently followed by the autoxidation of nitro radical anion and NAD(P)H-dependent reduction of NNOPs, resulting in Cu(II)-dependent redox cycle formation and DNA damage. This oxidative DNA damage may be supported by the report of Djuric et al. showing not only DNA adducts but also oxidative DNA damage in rats treated with 1,6-DNP (*8*).

Kohara et al. (*30*) showed that DNPs treatment increased the incidence of G → T transversions in mice. In this study, P450 reductase-treated DNPs induced Fpg sensitive sites preferentially at guanine residues and increased 8-oxodG formation. Shibutani et al. (*31*) have reported that 8-oxodG causes DNA misreplication, which can lead to mutation, particularly G → T substitutions. In addition, the bacterial mutation assay (*32*) revealed that DNPs exerted frequent base substitution mutations at cytosine residues. We demonstrated that NNOPs and P450 reductase-treated DNPs induced DNA cleavage sites preferentially at cytosine residues. Furthermore, piperidine and Fpg treatment detected cytosine and guanine damage of the ACG sequence complementary to codon 273, a well-known hotspot (*21*) of the *p53* gene. The occurrence of mutational hotspots may be partly explained by our observations. It is concluded that oxidative DNA damage, in addition to DNA adduct formation, may play important roles in the carcinogenesis of DNPs via metabolic activation on nitro group.

Acknowledgment. This work was supported by Grants-in-Aid for Scientific Research from the Ministry of Education, Science, Sports and Culture of Japan.

References

(1) IARC (1989) Diesel and gasoline engine exhausts and some nitroarenes. *IARC Monographs on the Evaluation of the Carcinogenic Risks to Humans*, Vol. 46, pp 1−373, IARC Press, Lyon.

(2) Watanabe, T., Hasei, T., Takahashi, Y., Otake, S., Murahashi, T., Takamura, T., Hirayama, T., and Wakabayashi, K. (2003) Mutagenic activity and quantification of nitroarenes in surface soil in the Kinki region of Japan. *Mutat Res. 538*, 121−131.

(3) Busby, W. F., Jr., Penman, B. W., and Crespi, C. L. (1994) Human cell mutagenicity of mono- and dinitropyrenes in metabolically competent MCL-5 cells. *Mutat Res. 322*, 233–242.
(4) Busby, W. F., Jr., Smith, H., Bishop, W. W., and Thilly, W. G. (1994) Mutagenicity of mono- and dinitropyrenes in the *Salmonella typhimurium* TM677 forward mutation assay. *Mutat. Res. 322*, 221–232.
(5) Steenland, K., Deddens, J., and Stayner, L. (1998) Diesel exhaust and lung cancer in the trucking industry: Exposure-response analyses and risk assessment. *Am. J. Ind. Med. 34*, 220–228.
(6) Carroll, C. C., Warnakulasuriyarachchi, D., Nokhbeh, M. R., and Lambert, I. B. (2002) *Salmonella typhimurium* mutagenicity tester strains that overexpress oxygen-insensitive nitroreductases nfsA and nfsB. *Mutat. Res. 501*, 79–98.
(7) Hilario, P., Yan, S., Hingerty, B. E., Broyde, S., and Basu, A. K. (2002) Comparative mutagenesis of the C8-guanine adducts of 1-nitropyrene and 1,6- and 1,8-dinitropyrene in a CpG repeat sequence. A slipped frameshift intermediate model for dinucleotide deletion. *J. Biol. Chem. 277*, 45068–45074.
(8) Djuric, Z., Potter, D. W., Culp, S. J., Luongo, D. A., and Beland, F. A. (1993) Formation of DNA adducts and oxidative DNA damage in rats treated with 1,6-dinitropyrene. *Cancer Lett. 71*, 51–56.
(9) Ohnishi, S., Murata, M., Fukuhara, K., Miyata, N., and Kawanishi, S. (2001) Oxidative DNA damage by a metabolite of carcinogenic 1-nitropyrene. *Biochem. Biophys. Res. Commun. 280*, 48–52.
(10) Heflich, R. H., Fifer, E. K., Djuric, Z., and Beland, F. A. (1985) DNA adduct formation and mutation induction by nitropyrenes in Salmonella and Chinese hamster ovary cells: Relationships with nitroreduction and acetylation. *Environ. Health Perspect. 62*, 135–143.
(11) Fifer, E. K., Heflich, R. H., Djuric, Z., Howard, P. C., and Beland, F. A. (1986) Synthesis and mutagenicity of 1-nitro-6-nitrosopyrene and 1-nitro-8-nitrosopyrene, potential intermediates in the metabolic activation of 1,6- and 1,8-dinitropyrene. *Carcinogenesis 7*, 65–70.
(12) Chumakov, P. (1990) EMBL Data Library, Accession Number ×54156.
(13) Serrano, M., Hannon, G. J., and Beach, D. (1993) A new regulatory motif in cell-cycle control causing specific inhibition of cyclin D/CDK4. *Nature 366*, 704–707.
(14) Capon, D. J., Chen, E. Y., Levinson, A. D., Seeburg, P. H., and Goeddel, D. V. (1983) Complete nucleotide sequences of the T24 human bladder carcinoma oncogene and its normal homologue. *Nature 302*, 33–37.
(15) Yamashita, N., Murata, M., Inoue, S., Hiraku, Y., Yoshinaga, T., and Kawanishi, S. (1998) Superoxide formation and DNA damage induced by a fragrant furanone in the presence of copper(II). *Mutat. Res. 397*, 191–201.
(16) Oikawa, S., Hirosawa, I., Hirakawa, K., and Kawanishi, S. (2001) Site specificity and mechanism of oxidative DNA damage induced by carcinogenic catechol. *Carcinogenesis 22*, 1239–1245.
(17) Yamamoto, K., and Kawanishi, S. (1989) Hydroxyl free radical is not the main active species in site-specific DNA damage induced by copper (II) ion and hydrogen peroxide. *J. Biol. Chem. 264*, 15435–15440.
(18) Murata, M., Mizutani, M., Oikawa, S., Hiraku, Y., and Kawanishi, S. (2003) Oxidative DNA damage by hyperglycemia-related aldehydes and its marked enhancement by hydrogen peroxide. *FEBS Lett. 554*, 138–142.
(19) Maxam, A. M., and Gilbert, W. (1980) Sequencing end-labeled DNA with base-specific chemical cleavages. *Methods Enzymol. 65*, 499–560.
(20) Ito, K., Inoue, S., Yamamoto, K., and Kawanishi, S. (1993) 8-Hydroxydeoxyguanosine formation at the 5′ site of 5′-GG-3′ sequences in double-stranded DNA by UV radiation with riboflavin. *J. Biol. Chem. 268*, 13221–13227.
(21) Levine, A. J., Momand, J., and Finlay, C. A. (1991) The p53 tumour suppressor gene. *Nature 351*, 453–456.
(22) Malaisse, W. J., Hutton, J. C., Kawazu, S., Herchuelz, A., Valverde, I., and Sener, A. (1979) The stimulus-secretion coupling of glucose-induced insulin release. XXXV. The links between metabolic and cationic events. *Diabetologia 16*, 331–341.
(23) Kukielka, E., and Cederbaum, A. I. (1994) Ferritin stimulation of hydroxyl radical production by rat liver nuclei. *Arch. Biochem. Biophys. 308*, 70–77.
(24) Ohnishi, S., Murata, M., and Kawanishi, S. (2002) Oxidative DNA damage induced by a metabolite of 2-naphthylamine, a smoking-related bladder carcinogen. *Jpn. J. Cancer Res. 93*, 736–743.
(25) Kawanishi, S., Hiraku, Y., Murata, M., and Oikawa, S. (2002) The role of metals in site-specific DNA damage with reference to carcinogenesis. *Free Radical Biol. Med. 32*, 822–832.
(26) Stiborova, M., Frei, E., Sopko, B., Sopkova, K., Markova, V., Lankova, M., Kumstyrova, T., Wiessler, M., and Schmeiser, H. H. (2003) Human cytosolic enzymes involved in the metabolic activation of carcinogenic aristolochic acid: Evidence for reductive activation by human NAD(P)H: quinone oxidoreductase. *Carcinogenesis 24*, 1695–1703.
(27) Ritter, C. L., and Malejka-Giganti, D. (1998) Nitroreduction of nitrated and C-9 oxidized fluorenes in vitro. *Chem. Res. Toxicol. 11*, 1361–1367.
(28) Djuric, Z., Potter, D. W., Heflich, R. H., and Beland, F. A. (1986) Aerobic and anaerobic reduction of nitrated pyrenes in vitro. *Chem.-Biol. Interact. 59*, 309–324.
(29) Djuric, Z. (1992) Comparative reduction of 1-nitro-3-nitrosopyrene and 1-nitro-6-nitrosopyrene: Implications for the tumorigenicity of dinitropyrenes. *Cancer Lett. 65*, 73–78.
(30) Kohara, A., Suzuki, T., Honma, M., Oomori, T., Ohwada, T., and Hayashi, M. (2002) Dinitropyrenes induce gene mutations in multiple organs of the lambda/lacZ transgenic mouse (Muta Mouse). *Mutat. Res. 515*, 73–83.
(31) Shibutani, S., Takeshita, M., and Grollman, A. P. (1991) Insertion of specific bases during DNA synthesis past the oxidation-damaged base 8-oxodG. *Nature 349*, 431–434.
(32) Watanabe, T., Takashima, M., Kasai, T., and Hirayama, T. (1997) Comparison of the mutational specificity induced by environmental genotoxin nitrated polycyclic aromatic hydrocarbons in *Salmonella typhimurium* his genes. *Mutat. Res. 394*, 103–112.

TX0497550

in vivo 18: 561-570 (2004)

1-Amino-4-phenyl-1,2,3,6-tetrahydropyridine and 1-Amino-4-phenylpyridinium Salt, the 1-Amino Analogues of Neurotoxins, MPTP and MPP+, Induce Apoptosis in PC12 Cells: Detection of Apoptotic Cells by Comet Assay and Flow Cytometric Analysis

YASUHIRO NODA, TOMOE SUMINO, YUKI FUJISAWA, NAOKI MIYATA, TOYO KAIYA and KOHFUKU KOHDA

Graduate School of Pharmaceutical Sciences, Nagoya City University, Tanabedori, Mizuho-ku, Nagoya 467-8603, Japan

Abstract. *1-Methyl-4-phenyl-1,2,3,6-tetrahydropyridine (MPTP) is known to induce parkinsonism in humans when it is oxidized to the 1-methyl-4-phenylpyridinium salt (MPP^+). We previously reported the syntheses of 1-amino-4-phenyl-1,2,3,6-tetrahydropyridine (APTP) and 1-amino-4-phenyl-pyridinium salt (APP^+), the 1-amino analogues of the dopaminergic neurotoxins, MPTP and MPP^+, respectively, and demonstrated that both APTP and APP^+ are cytotoxic to PC12 cells. In this study, we found that both APTP and APP^+ induce apoptotic cell death in PC12 cells. Apoptosis was determined by the Comet assay and flow cytometric analysis. Prior to using the Comet assay for detection of apoptotic PC12 cells, Comet images of apoptotic and necrotic cells were first distinguished by using several standards. Comet images were classified into four groups (A to D) according to their shapes. Class D consisted of the apoptotic cells and was easily distinguished. We also demonstrated that apoptotic and necrotic PC12 cells can be easily differentiated and quantified using the convenient Comet assay.*

1-Methyl-4-phenyl-1,2,3,6-tetrahydropyridine (MPTP) is known to induce parkinsonism in humans when it is oxidized to the 1-methyl-4-phenylpyridinium salt (MPP^+) (1). (Figure 1). We previously synthesized 1-amino-4-phenyl-1,2,3,6-tetrahydropyridine (APTP) and 1-amino-4-phenylpyridinium salt (APP^+), the 1-amino analogues of the dopaminergic neurotoxins, MPTP and MPP^+, respectively, and reported that both APTP and APP^+ were cytotoxic to PC12 cells, while only MPP^+ was cytotoxic in the methyl analogue (2). These differences were supported by the fact that APTP is oxidized to the active form, APP^+, by MAO-A in PC12 cells, while MPTP can be oxidized to the active form MPP^+ by MAO-B, which does not exist in these cells (3). It is reported that the cytotoxic effect of MPP^+ is caused by the induction of apoptosis (4), however, no studies have been done on APTP and APP^+.

We conducted this investigation to determine whether apoptosis is involved in the cell death induced by APTP and APP^+, as it is with MPP^+. For detection of apoptosis, both the Comet assay and flow cytometric analysis were employed. The Comet assay is a convenient and useful method for detecting DNA degradation and apoptosis (5-8), however, only a few reports have been published describing DNA damage in PC12 cells (9, 10) and none describing the detection of apoptosis. In this study, we first determined the Comet image of apoptotic cells in order to establish the method. Using this system together with flow cytometric analysis, we confirmed that both APTP and APP^+ induce apoptosis in PC12 cells, as does MPP^+.

Materials and Methods

Materials. Propidium iodide, 4',6-diamidino-2-phenylindole (DAPI), trypsin and RNase A were purchased from Sigma Chemical Co., Ltd. (St. Louis, MO, USA), agarose gel was from Nacalai Tesque, Inc. (Kyoto, Japan), proteinase K, Tris, EDTA and sodium laurylsarcosinate were from Wako Pure Chemical Industries, Ltd. (Osaka, Japan), ethidium bromide was from Aldrich Chemical Co., Inc. (Tokyo, Japan), and the Annexin V-FITC kit was from Trevigen, Inc. (Gaithersburg, MD, USA). The phosphate-buffered saline (PBS) used was Dulbecco's PBS. Flow cytometric analysis was carried out with a FACSort (Becton Dickinson, USA).

Correspondence to: Dr. Kohfuku Kohda, Faculty of Pharmaceutical Sciences, Musashino University, Shinmachi, Nishitokyo-shi, Tokyo 202-8585, Japan. e-mail: kohda@musashino-u.ac.jp

Key Words: PC12 cells, neurotoxin, MPP^+, APP^+, apoptosis, Comet assay.

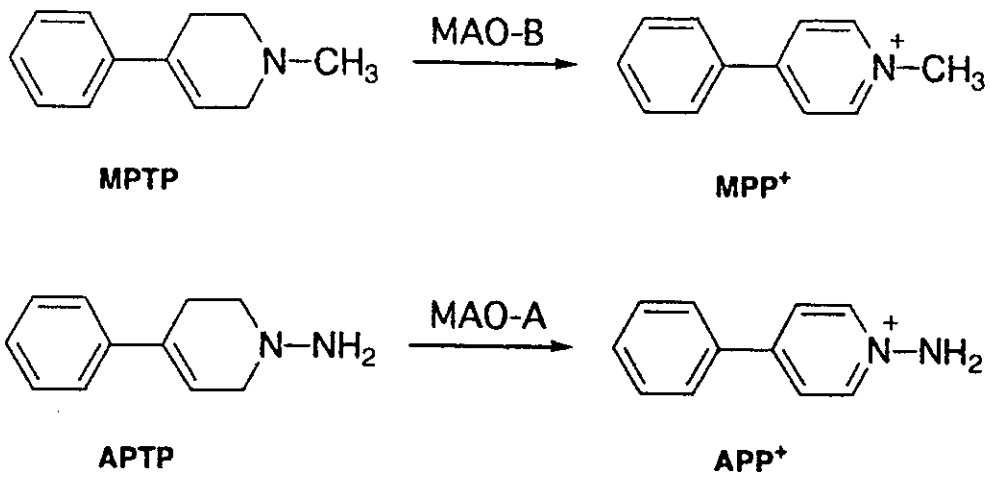

Figure 1. *Structures of MPTP, MPP+, APTP and APP+.*

Cell culture. Rat phenochromocytoma PC12 cells were cultured in Dulbecco's modified Eagle medium (Nissui Pharmaceutical Co., Ltd., Tokyo, Japan) supplemented with 10% horse serum (Nacalai Tesque Inc., Kyoto, Japan), 5% fetal bovine serum (Summit Biotechnology Co., Ltd., Fort Collins, CO, USA) and 0.1 mg/ml kanamycin (Meiji Seika Co., Ltd., Tokyo, Japan) under a humidified atmosphere of 5% CO_2 in air at 37°C.

Flow cytometric analysis of cells in the sub-G1 region. We used a previously reported method with a slight modification (11). Cells (2 x 10^6) were seeded in a 50-mm plastic dish containing 5 ml medium and pre-cultured for 24 h. The test compound (50 μl) dissolved in DMSO was added and the cells were incubated for a specified time. The medium was then removed and the cells were washed with 2 ml of 0.02% EDTA in PBS. After the cells had been detached with 1 ml of 0.125% trypsin solution (0.02% EDTA in PBS), 5 ml of medium was added and the cells were collected by centrifugation. They were then washed with 1 ml of PBS, resuspended in 1 ml of cold 70% ethanol and refrigerated for 30 min. Cells were collected by centrifugation and washed with 1 ml of PBS. The cell pellet was treated with 50 μl of RNase A solution (1 mg/ml PBS) and 500 μl of disodium hydrogenphosphate-citric acid buffer (prepared by mixing 192 ml of 0.2 M Na_2HPO_4 and 8 ml of 0.1 M citric acid), and the mixture was incubated at 37°C for 30 min. Then, the cells were stained for 30 min at room temperature in the dark, after addition of a further 500 μl of disodium hydrogenphosphate-citric acid buffer and 50 μl of propidium iodide solution (1mg/ml H_2O). This cell suspension was passed through a nylon mesh and subjected to flow cytometric analysis of the sub-G1 region.

Flow cytometric analysis of cells in early apoptosis. An Annexin V-FITC kit was used according to the manufacturer's instructions. After the cells were treated with the test compound for 30 h, they were collected as described above. To the cell pellet (1 x 10^6 cells) was added 100 μl of Annexin V incubation reagent (which contains Annexin V conjugate and propidium iodide, prepared according to the manufacturer's instructions), and the cells were incubated for 15 min at room temperature in the dark. After a binding buffer (400 μl) had been added, the cell suspension was passed through a nylon mesh and subjected to flow cytometric analysis.

Comet assay. Our previously reported method was used (12-14). Cells were collected by centrifugation, washed with PBS and resuspended in 500 μl of PBS. Twenty μl of the cell suspension was then mixed with 140 μl of 1% low melting temperature agarose gel. A hundred μl aliquot of this mixture was rapidly pipetted onto frosted microscope slides and allowed to gel at 4°C for 10 min. The slides were then immersed in lysis solution (2.5 M NaCl, 100 mM EDTA, 10 mM Tris-HCl buffer (pH 10), 1% sodium sarcosinate with 1% Triton X-100 and 10% DMSO) at 4°C for 1 h, then placed in a high pH electrophoresis buffer (1 mM EDTA, 300 mM NaOH) at 4°C for 20 min before electrophoresis. Electrophoresis was conducted at 4°C for 20 min at 25 V and 300 mA. The slides were then immersed twice in 0.4 M Tris-HCl buffer (pH 7.5) for 5 min each time, stained with DAPI (1 μg/ml) and covered with coverslips. Comet images were observed at more than 200x magnification with a fluorescence microscope (BX60, Olympus Co., Tokyo, Japan) attached to a video camera (CCD X-2, Shimadzu Rika Instruments, Tokyo, Japan) connected to a display screen. Fifty images were randomly selected from each sample and their Comet lengths were measured on the screen and classified as A to D. The extent of DNA strand breakage was evaluated by comparing the population of class A to D to that of the control cells.

DNA gel electrophoresis. DNA fragmentation was monitored by agarose gel electrophoresis. A previously reported method was used with a slight modification (15). Cells (1 x 10^6) were washed with cold PBS, centrifuged at 4°C and resuspended in 20 μl of 50 mM Tris-HCl (pH 8.0) containing 10 mM EDTA, 0.5% (w/v) sodium laurylsarcosinate and 0.5 mg/ml proteinase K. After 1-h incubation at 50°C, 10 μl of 0.5 mg/ml RNase A was added. Incubation at 50°C was continued for an additional hour followed by heating to 70°C. The cell suspension was then mixed with 10 μl of 10 mM EDTA (pH 8.0) containing 1% (w/v) low melting temperature agarose,

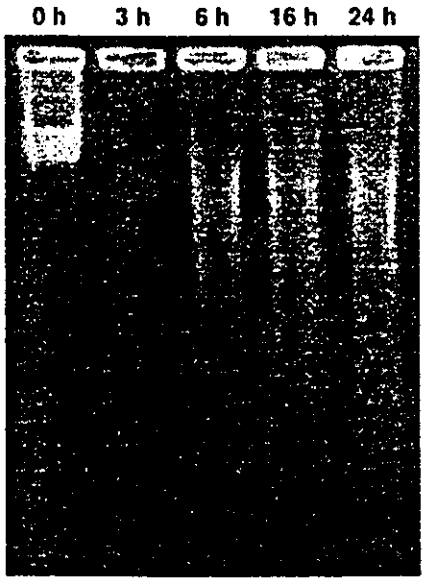

Figure 2. *Gel electrophoresis of PC12 cells starved for 3, 6, 16 and 24 h.*

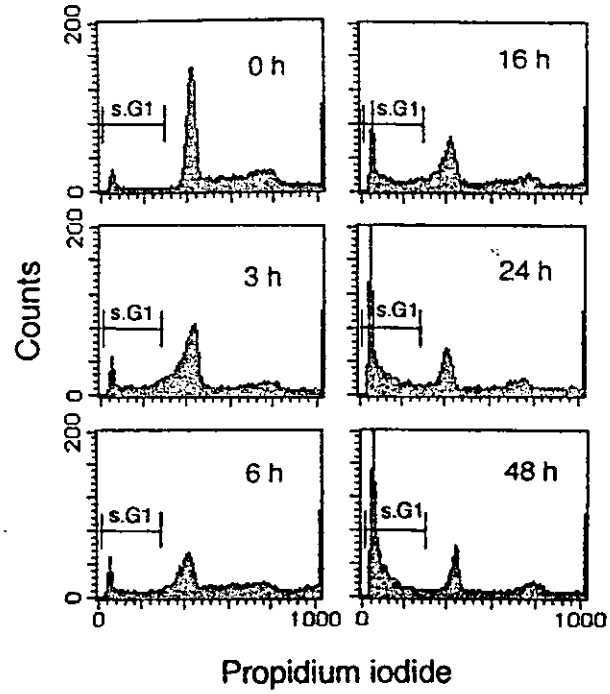

Figure 3. *Flow cytometry of PC12 cells starved for 3, 6, 16, 24 and 48 h. Detection of cells in the sub-G1 region. s.G1 shown in figure denotes the sub-G1 region.*

0.25% (w/v) bromophenol blue and 40% (w/v) sucrose, and loaded into wells prepared on a 1.2% (w/v) high melting temperature agarose gel plate. Electrophoresis was carried out at a voltage of 100 V in 2 mM EDTA–89 mM Tris-borate (pH 8.0) until the marker dye had migrated a distance of 3 ~ 4 cm. The agarose gel was then stained for 10 min with 0.1 μg/ml ethidium bromide.

Results and Discussion

The Comet assay (5-8), a microelectrophoresis technique, is a useful method for detecting DNA fragmentation in cells and widely used for the detection of DNA damage caused by mutagens/carcinogens. Our decision to use this method to analyze apoptotic PC12 cells was based on the fact that it proved satisfactory in our previous study (12-14). However, no report has been published on the detection of apoptosis in PC12 cells using the Comet assay. In this assay, Comet-like images with a head and tail can be observed, while the extent of DNA migration depends on the degree of DNA fragmentation. The DNA of apoptotic cells is fragmented by endonuclease, however, it was not clear which Comet image corresponded to the apoptotic cells. In order to ascertain this, apoptotic PC12 cells were prepared by a method in which the cells were cultured in a serum-deprived medium (16). To verify that apoptosis had been initiated, starved cells were analyzed by both agarose gel electrophoresis and flow cytometry and the induction of apoptosis was confirmed by the appearance of the ladder pattern (Figure 2) and the sub-G1 peak (Figure 3), respectively, which are characteristic of apoptotic cells. Starved cells were then subjected to the Comet assay. In order to compare these images with the typical Comet images induced by non-apoptotic cell death, cells treated with *N*-methyl-*N*-nitrosourea (MNU) were also subjected to the Comet assay (8). The Comet images observed with PC12 cells after starvation and treatment with MNU under several types of conditions were classified into four groups (A to D) as shown in Figure 4. Comet length was measured as the full length of the Comet, including the nucleus (the head portion) and tail, after electrophoresis. For comparison, the size of the Comet was expressed as the ratio of the full Comet length relative to the diameter of a normal nucleus. Figure 4-A shows the Comet image of control cells in which no, or a very small, tail can be observed, the size of the Comet being less than 1.2. Figure 4-B shows the appearance of a distinct tail and reduced nucleus, the size of the Comet being from 1.2 to 2.5. Figure 4-C shows a Comet with a big tail and a size of more than 2.5. The Comet images shown in Figures 4-B and 4-C were particularly characteristic of PC12 cells treated with MNU, as described later. Figure 4-D shows a highly diffused elliptical Comet tail and regression of the nucleus that may have been caused by extensive DNA degradation. This is a typical Comet image obtained with starved cells, and the cells in class D were determined to be

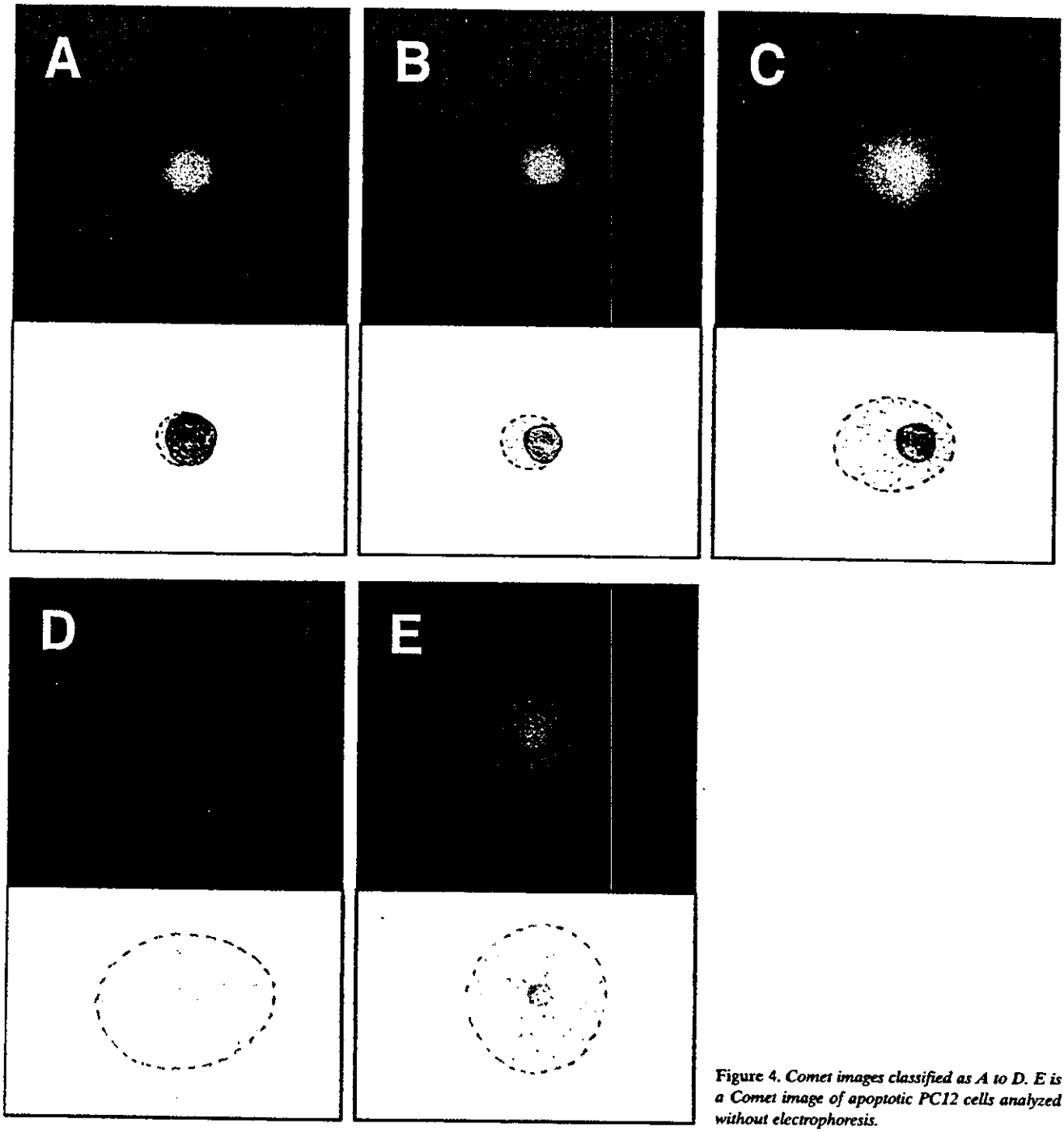

Figure 4. *Comet images classified as A to D. E is a Comet image of apoptotic PC12 cells analyzed without electrophoresis.*

apoptotic. Although the brightness of the Comet images of class D was weaker than that of the images of Figures 4-A to 4-C because of the high diffusion of the DNA fragments, these images are easily distinguishable from the Comet images of other cells with higher magnification (more than 200x). Furthermore, when the Comet assay was carried out without electrophoresis, a more typical image of apoptotic cells was observed, as shown in Figure 4-E, in which small DNA fragments are scattered around a small nucleus. This type of image was similar to that observed in the diffusion assay used by Singh (17) for the estimation of apoptotic cells.

Using this classification system, the population of cells was placed into class A to D after starvation and MNU treatment. Figure 5 shows the results of cells starved for 0 to 24 h. The

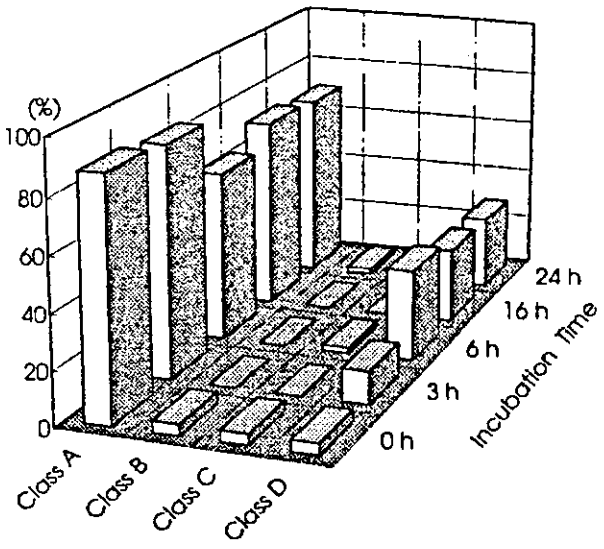

Figure 5. *Population of PC12 cell classified as A to D after cells were starved for the indicated times.*

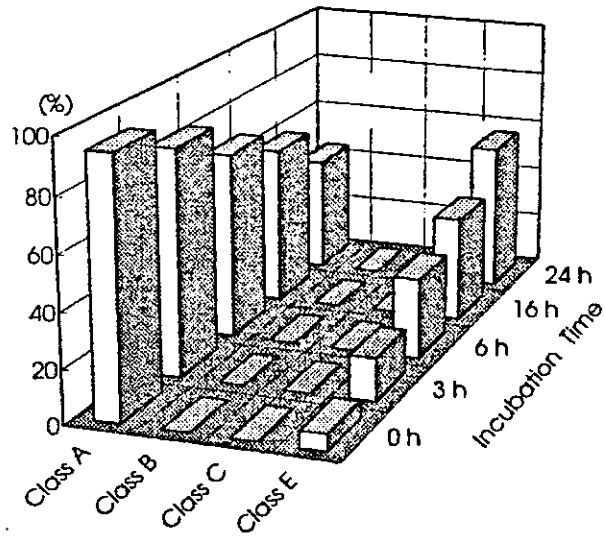

Figure 6. *Population of PC12 cells classified as A to C and D after cells were starved for the indicated times. The Comet assay was carried out without electrophoresis.*

population of cells in class D increased with time up to 6 h, then slightly decreased with further starvation. When the Comet assay was performed without electrophoresis, very clear results were obtained; only cells in class A (only the nucleus was seen) and class E were observed, and the population of cells in class E increased while that in class A decreased with ongoing starvation (Figure 6). Results for cells treated with MNU for 24 h are shown in Figure 7. Cells in class B became most numerous with 2 mM MNU treatment, while cells in class C increased with increasing MNU doses, reaching their highest level with the 4 mM dose. Cells in class D increased with an increasing dose, however, their numbers were very low. In the case of MNU-treated cells, when the Comet assay was carried out without electrophoresis, it was difficult to distinguish cells in class E from cells in other classes. Therefore, for detection of apoptotic cells, the Comet assay with electrophoresis is preferred.

Using this system, induction of apoptosis by APP$^+$ and APTP was analyzed together with induction by MPP$^+$. Figure 8 shows the results obtained with PC12 cells treated with MPP$^+$, APP$^+$ and APTP for 24 h. In every case, only the population of cells in class D increased with an increasing dose. For APTP, a high dose was required to give a population similar to that of cells treated with MPP$^+$ and APP$^+$. These results corresponded to those of our previous report showing that the cytotoxic effect of APTP on PC12 cells is weaker than that of APP$^+$ using a shorter treatment time (2).

For induction of apoptosis by MPP$^+$, APP$^+$ and APTP, other detection methods, such as flow cytometric analysis,

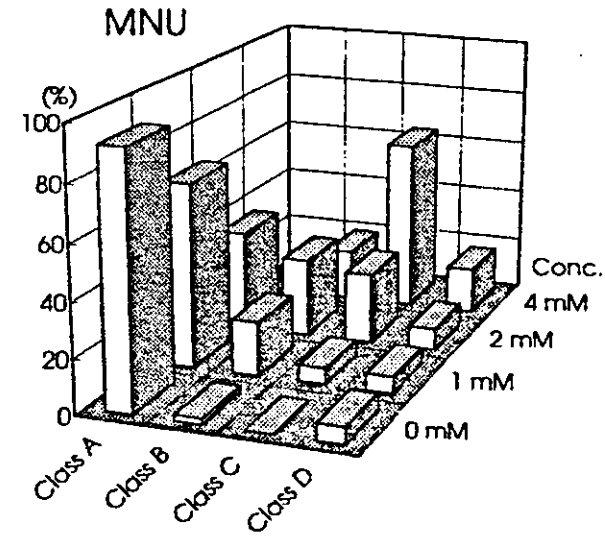

Figure 7. *Population of PC12 cells classified as A to D after cells were treated with MNU (1, 2, and 4 mM) for 24 h.*

were also applied. After cells had been treated with APP$^+$ or APTP at doses of 0.125, 0.5 and 1 mM, induction of apoptotic cell death was analyzed by flow cytometry. Two methods were used; analyses of cells i) in the sub-G1 region using propidium iodide and ii) in early apoptosis using an Annexin V-FITC kit. As a positive control, MPP$^+$ was also

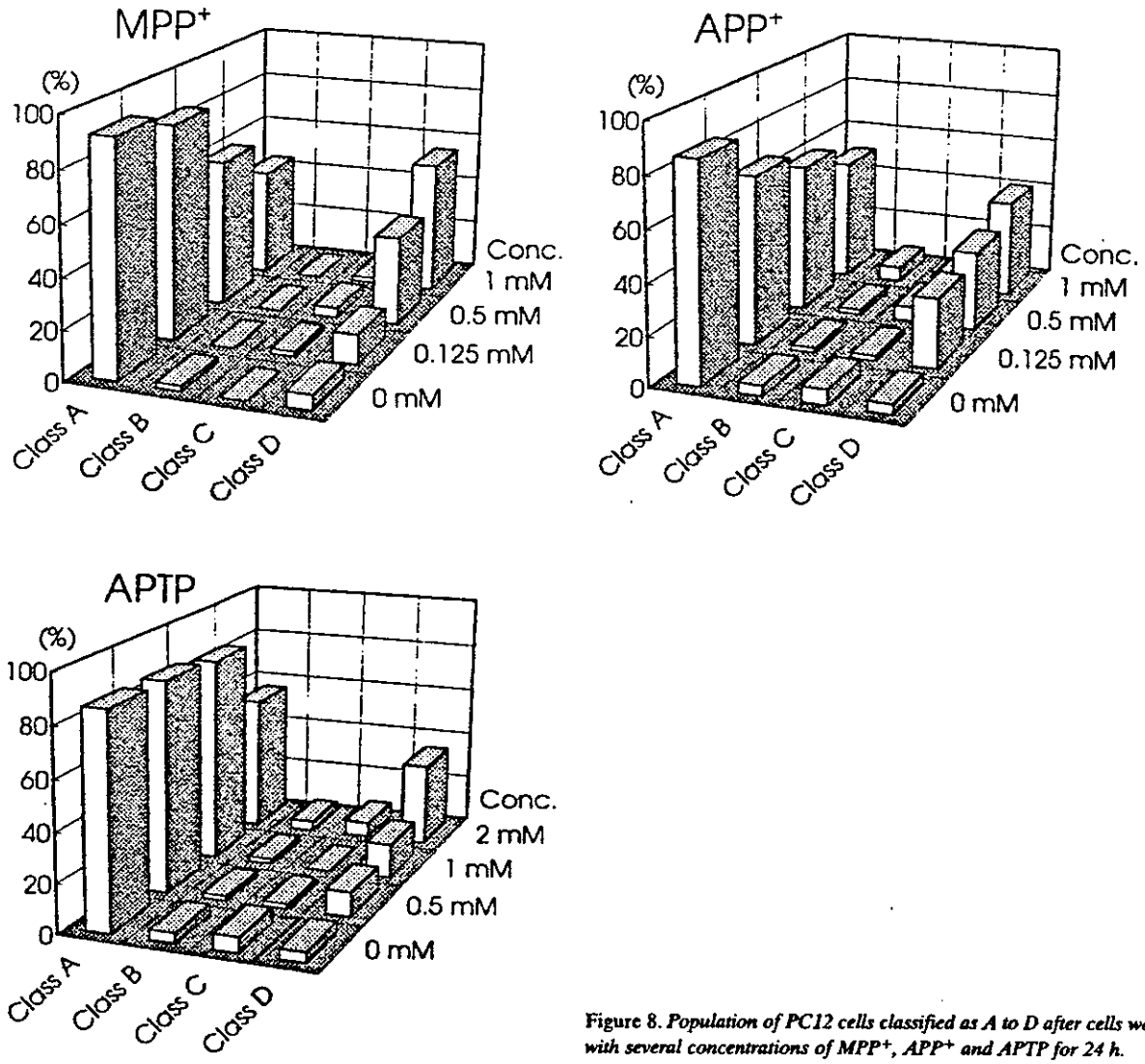

Figure 8. *Population of PC12 cells classified as A to D after cells were treated with several concentrations of MPP+, APP+ and APTP for 24 h.*

used. Flow cytometric data for the sub-G1 region after 48 h of treatment are shown in Figure 9. The percentages of cells in the sub-G1 region were calculated and summarized in Table I. With the MPP^+ treatment, the fractions of cells in the sub-G1 region increased with an increasing dose. Results of APP^+ and APTP were quite similar to those for MPP^+. This indicates that induction of apoptosis occurs with APP^+ and APTP as it does with MPP^+. Flow cytometric data on cells in early apoptosis after 30-h treatment are shown in Figure 10. With MPP^+, the cell population shifted from the lower left (LL) to lower right (LR), the state of early apoptosis, with an increasing treatment dose, and it then shifted further to the upper right (UR), the state of late apoptosis. The cell population shifted similarly with APP^+ and APTP. Cell populations in LL, LR and UR quadrants at each dose are summarized in Table II. With APP^+, the population shifted from LL to LR with an increasing dose, however, it required a very high dose to give a cytometric pattern similar to that of APTP. These results corresponded to those of our previous report showing that the cytotoxicity of APTP towards PC12 cells is stronger than that of APP^+ with a longer treatment time (2). From these results, we concluded that both APP^+ and APTP induce apoptosis in PC12 cells as does MPP^+.

In the Comet assay, apoptotic cells could be detected at 24 h after cells were treated with MPP^+, APP^+ or APTP as shown in Figure 8, while with flow cytometric analysis using an Annexin V-FITC kit, early apoptotic cells were observed

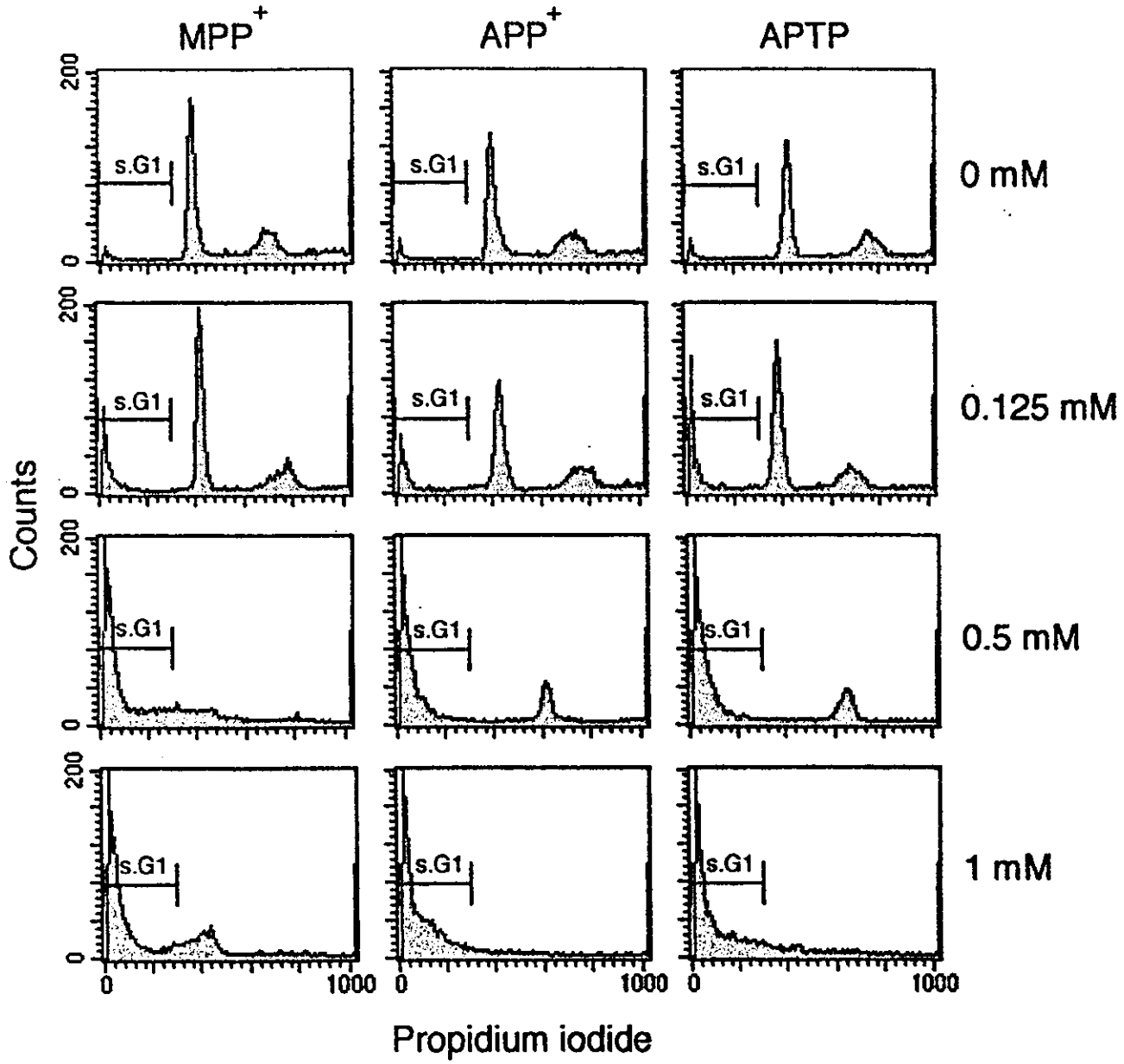

Figure 9. *Flow cytometry of PC12 cells treated with several concentrations of MPP+, APP+ and APTP for 48 h. Detection of cells in the sub-G1 region. s.G1 shown in figure denotes the sub-G1 region.*

only in the case of MPP^+. For APP^+ and APTP, early apoptotic cells were not observed at 24 h of treatment but did appear after 30 h, as shown in Figure 10. These results indicated that the Comet assay is a more sensitive method for detecting cells in early apoptosis than is flow cytmetric analysis using an Annexin V-FITC kit.

Apoptosis, programmed cell death, can be detected by several methods such as flow cytometric analysis (11), agarose gel electrophoresis (15), the TUNEL assay (18) and others. The Comet assay is also known to be a convenient

Table I. *Fraction of cells in the sub-G1 region*.*

Conc (μM)	% MPP+	APP+	APTP
0	1.0	1.7	1.8
125	12.4	10.8	14.1
500	75.4	61.2	65.1
1,000	66.7	84.6	77.1

*Cells were treated with MPP+, APP+ or APTP for 48h

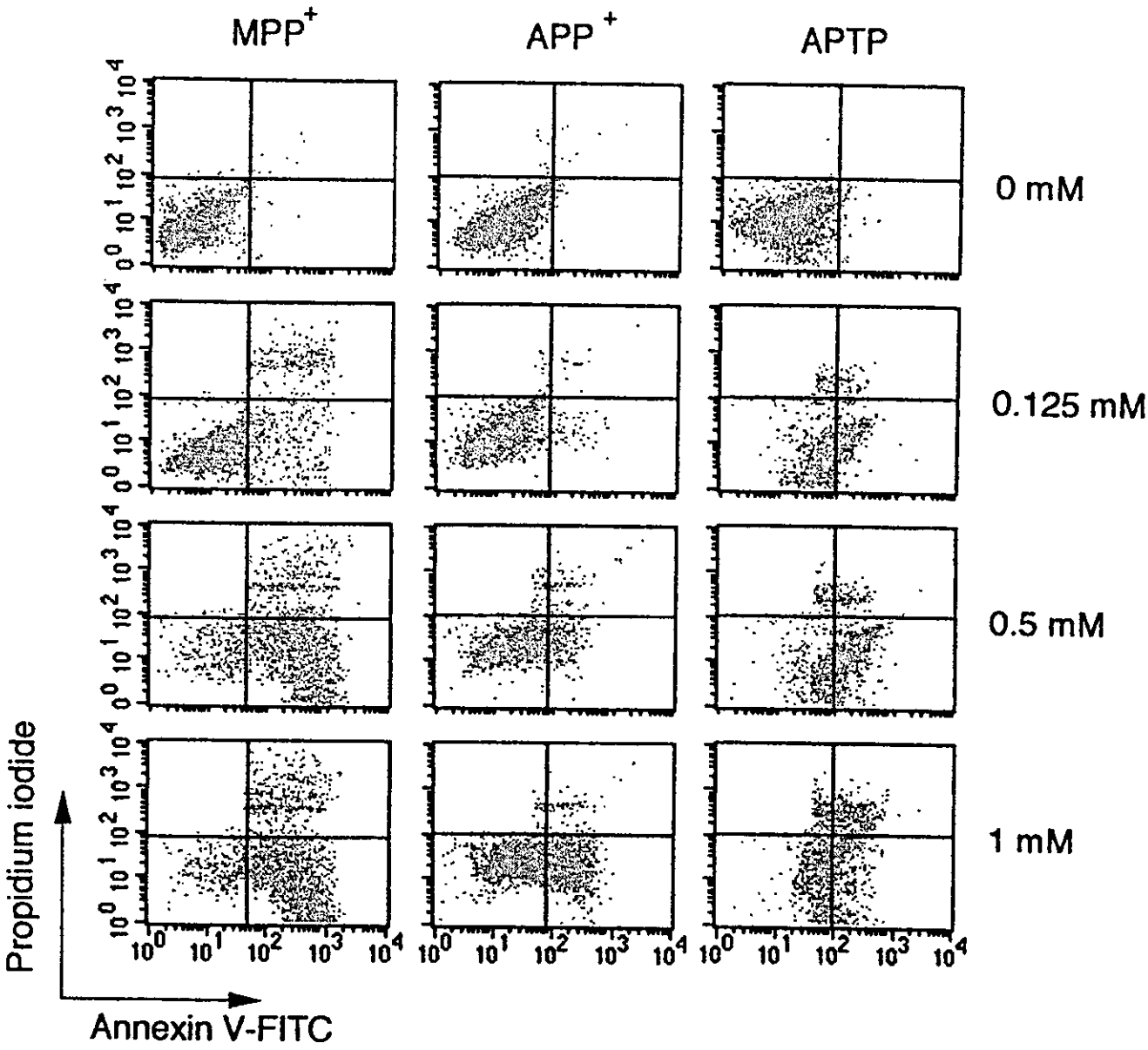

Figure 10. *Detection of cells in the early apoptotic state by flow cytometry. Cells were treated with several concentrations of MPP+, APP+ and APTP for 30 h.*

method for detecting DNA degradation including apoptosis (5, 6), however, very few reports have been published on DNA damage of PC12 cells. Furthermore, no studies have appeared on the detection of apoptosis in PC12 cells using the Comet assay. We modified the Comet assay to establish the procedures for determining apoptosis in these cells. Since PC12 cells are used widely as models of nerve cells, our method for performing the Comet assay should prove to be convenient for distinguishing and quantifying both apoptotic and necrotic cells.

References

1 Langston J W, Ballard P, Tetrud J W and Irwin I: Chronic parkinsonism in humans due to a product of meperidine-analog synthesis. Science *219*: 979-980, 1983.

2 Kohda K, Noda Y, Aoyama S, Umeda M, Sumino T, Kaiya T, Maruyama W and Naoi M: Cytotoxicity of 1-amino-4-phenyl-1,2,3,6-tetrahydropyridine and 1-amino-4-phenylpyridinium ion, 1-amino analogues of MPTP and MPP+, to clonal pheochromocytoma PC 12 cells. Chem Res Toxicol *11*: 1249-1253, 1998.

Table II. *Cells in LL, LR and UR quadrants*.*

Conc (μM)		% MPP+	APP+	APTP
0	LL	98.4	98.2	97.5
	LR	0.4	0.9	1.2
	UR	0.4	0.6	0.2
125	LL	77.3	95.7	67.3
	LR	10.8	2.2	32.5
	UR	10.8	0.7	0.2
500	LL	15.4	79.0	36.3
	LR	62.3	11.4	62.9
	UR	20.0	4.8	0.8
1,000	LL	12.0	49.4	45.1
	LR	56.2	43.9	34.1
	UR	25.0	4.3	20.8

* Cells were treated with MPP+, APP+ or APTP for 30 h, and flow cytometry was carried out using Annexin V and propidium iodide staining. LL; lower left, LR; lower right, UR; upper right

3 Umeda M, Aoyama S, Kaiya T, Kohda K, Maruyama W and Naoi M: Oxidation of 1-amino-4-phenyl-1,2,3,6-tetrahydropyridine, a 1-amino analogues of MPTP, by type A and B monoamine oxidase. J Neural Transm *105*: 1253-1264, 1998.

4 Dipasquale B, Marini AM and Youle RJ: Apoptosis and DNA degradation induced by 1-methyl-4-phenylpyridinium in neurons. Biochem Biophys Res Commun *181*: 1442-1448, 1991.

5 Collins AR: The Comet assay: Principles, applications, and limitations. *In*: *In situ* detection of DNA damage: Methods and protocols. "Methods in Molecular Biology" Vol. 203: (Didenko VV, ed). Totowa NJ, Human Press Inc, 2002, pp 163-177.

6 Olive PL: The Comet assay: An overview of techniques. *In*: *In situ* detection of DNA damage: Methods and protocols. "Methods in Molecular Biology" Vol. 203: (Didenko VV, ed). Totowa NJ, Human Press Inc, 2002, pp 179-194.

7 Yasuhara S, Zhu Y, Matsui T, Tipirneni N, Yasuhara Y, Kaneki M, Rozenzweig A and Martyn JA: Comparison of Comet assay, electron microscopy, and flow cytometry for detection of apoptosis. J Histochem *51*: 873-885, 2003.

8 Roser S, Pool-Zobel B-L and Rechkemmer G: Contribution of apoptosis to responses in the Comet assay. Mut Res *497*: 169-175, 2001.

9 Martin D, Salinas M, Fujita N, Tsuruo T and Cuadrado A: Ceramide and reactive oxygen species generated by H_2O_2 induce caspase-3-independent degradation of Akt/protein kinase B. J Biol Chem *277*: 42943-42952, 2002.

10 Wang L, Nishida H, Ogawa Y and Konishi T: Prevention of oxidative injury in PC12 cells by a traditional Chinese medicine, Shengmai San, as a model of an antioxidant-based composite formula. Biol Pharm Bull *26*: 1000-1004, 2003.

11 Darzynkiewicz Z, Bruno S, Del Bino G, Gorczyca W, Horz MA, Lassota P and Traganos F: Features of apoptosis cells measured by flow cytometry. Cytometry *13*: 795-808, 1992.

12 Kasamatsu T, Kohda K and Kawazoe Y: Cytotoxicity of antitumor agents toward cultured murine leukemia L1210 cells under a serum-deprived apoptotic condition. Anticancer Res *15*: 2597-2600, 1995.

13 Kasamatsu T, Kohda K and Kawazoe Y: Comparison of chemically induced DNA breakage in cellular and subcellular systems using the Comet assay. Mutat Res *369*: 1-6, 1996.

14 Kasamatsu T, Kohda K and Kawazoe Y: Synergetic cytotoxicity of bleomycin and polyhydric alcohols: DNA strand breakage evaluated by "Comet assay". Biol Pharm Bull *19*: 632-635, 1996.

15 Smith CA, Williams GT, Kingston R, Jenkinson EJ and Owen JJT: Antibodies to CD3/T-cell receptor complex induce death by apoptosis in immature T cells in thymic cultures. Nature *337*: 181-184, 1989.

16 Lindenboim L, Diamond R, Rothenberg E and Stein R: Apoptosis induced by serum deprivation of PC12 cells is not preceded by growth arrest and can occur at each phase of the cell cycle. Cancer Res *55*: 1242-1247, 1995.

17 Singh NP: A simple method for accurate estimation of apoptotic cells. Exp Cell Res *256*: 328-337, 2000.

18 Loo DT: TUNEL assay: An overview of techniques. *In*: *In situ* detection of DNA damage: Methods and protocols. "Methods in Molecular Biology", Vol. 203: (Didenko VV, ed). Totowa NJ, Human Press Inc, 2002, pp 21-30.

Received June 16, 2004
Accepted July 8, 2004

Polycyclic Aromatic Compounds, 24: 487–500, 2004

ISSN: 1040-6638 print / 1563-5333 online
DOI: 10.1080/10406630490471500

Taylor & Francis
Taylor & Francis Group

ASSOCIATIONS BETWEEN CHEMICAL PROPERTIES AND OXIDATIVE DAMAGE DUE TO NITROPHENANTHRENES AND THEIR RELATED COMPOUNDS IN PRIMARY RAT HEPATOCYTES

Nobuyuki Sera
Fukuoka Institute of Health and Environmental Sciences, Dazaifu, Fukuoka, Japan
Hiroshi Tokiwa
Laboratory of Environmental Health Science, Kyushu Women's University, Yahatanishi-ku, Kitakyushu, Japan
Hideo Utsumi
Laboratory of Bio-Fuction Analysis, Graduate School of Pharmaceutical Sciences, Kyushu University, Higashi-ku, Fukuoka, Japan
Shigeki Sasaki
Bioorganic and Synthetic Chemistry, Graduate School of Pharmaceutical Sciences, Kyushu University, Higashi-ku, Fukuoka, Japan
Kiyoshi Fukuhara
Naoki Miyata
National Institute of Health Sciences, Setagaya-ku, Tokyo, Japan

Nitrated derivatives of phenanthrene, azaphenanthrene, and their N-oxides were synthesized, and their chemical properties, LUMO energy, the first and second reduction potentials, and dihedral angle of nitro groups were investigated. On orientation of 22 nitrophenanthrenes (NPhs), and 19 nitroazaphenanthrenes (NAPhs) containing their N-oxides (NPhOs), NPhs and NAPhs substituted at positions 2, 3, 6, and 7 were almost coplanar to the

Received 1 September 2003; accepted 1 February 2004.
Address correspondence to Nobuyuki Sera, Fukuoka Institute of Health and Environmental Sciences, 39 Mukaizano Dazaifu, Fukuoka 818-0135, Japan. E-mail: sera@fihes.pref.fukuoka.jp

aromatic ring, while those at positions 1, 5, 8, 9, and 10 were almost perpendicular. On the other hand, primary rat hepatocytes prepared from SD rats efficiently induced 8-oxodeoxyguanine (8-oxo-Gua) of 4-nitroquinoline N-oxide (4-NQO), a mutagen and carcinogen. 8-oxo-Gua formed due to oxidative damage was dose dependent at levels from 1.0 to 5.0 nM of 4-NQO. 8-oxo-Gua formation of NPhs and NAPhs in primary rat hepatocytes was determined, and the results significantly correlated with the first reduction potentials (r = 0.906) and LUMO energy (r = 0.874) of these derivatives. It was concluded that the nitro group of Phs and APhs were metabolized by the NADPH-cytochrome p450 enzyme in primary rat hepatocytes, and a radical anion of NPhs was induced. Finally, the hydroxyl radicals induced promoted hydroxylation at the 8 position of the guanine residue. It was found that these metabolic pathways were closely associated with the first reduction potentials, and the LUMO energy of NPhs and NAPhs, as well as 8-oxo-Gua formation were related to these chemical properties.

Keywords nitroazaphenanthrenes, nitrophenanthrenes, 8-oxodeoxyguanosine

Many investigators have discussed the association between the mutagenicity of nitrated polycyclic aromatic hydrocarbons (nPAHs) and their chemical structure (1–9). Nitrophenanthrene derivatives are ubiquitous mutagens in the environment, and distribute widely in diesel exhaust particulates (10). We have already reported that there was a relationship between *Salmonella* mutagenicity and orientation of nitrophenanthrenes (9) and nitroazaphenanthrenes (11). For *Salmonella* mutagenicity of nitrophenanthrenes (NPhs), nitro substituents that were almost coplanar in aromatic rings enhanced mutagenicity while those which were perpendicular in the rings reduced this activity (9–11). It was revealed that the mutagenic activity of NPhs was closely associated with reduction potentials and the dihedral angles of the nitro substituent for intercalation of chemicals into DNA (9, 11).

On the other hand, 8-hydroxyguanosine has been used as a biomarker of oxidative DNA damage in human lung tissue (12, 13), human leukocytes (14), and in the urinary tract (15). Furthermore, it was found that environmental substances such as diesel particles formed 8-hydroxyguanine in an in vivo test in mice, and that they were involved

in the generation of oxygen and hydroxyl radicals through phagocytosis of particles in macrophages (16).

In this study, it was demonstrated that there was a correlation between 8-oxodeoxyguanosine (8-oxo-Gua) formed in primary rat hepatocytes and the chemical properties of NPhs and their related compounds. It was found that the first reduction potentials and LUMO energy of nPAHs may be involved with 8-oxo-Gua formation through radical reactions in metabolic pathways.

MATERIALS AND METHODS

Chemicals

Nitrophenanthrenes (NPhs) used were 1-, 3-, and 9-NPhs; 1,5-, 1,6-, 1,10-, 2,6-, 2,9-, 2,10-, 3,5-, 3,6-, 3,10-, 4,9-, and 4,10-diNPhs; and 1,5,9-, 1,5,10-, and 3,6,9-triNPhs as reported previously (9). Nitroazaphenanthrenes (NAPhs) used were 8-nitro-1-azaphenanthrene (8-N-1-APh), 6- and 8-N-4-APhs, 4-, 5-, 6-, and 7-N-9-APhs, 5-, 6-, and 8-N-1-APh N-oxide (5-, 6-, and 8-N-1-APhO), 5-, 6-, and 8-N-4-APhOs, 1-, 2-, 3- and 5-N-9-APhOs, and 1,5- and 1,8-dinitro-4-APhOs (1,5- and 1,8-diN-4-APhOs) as reported previously (11, 17). 4-Nitroquinolin-N-oxide (4-NQO) was obtained from Sigma Chemical Company.

Electrochemical Reduction by Cyclic Voltammetry and Electronic Descriptors

The electronic descriptor and LUMO energy levels of chemicals were calculated by MOPAC 2002 (AM1), which is based on the MOPAC of the Toray System Center, using the AM1 method. The initial geometries were constructed from standard bond lengths and angles. The geometries were then completely optimized using algorithms in the MOPAC program. Electrochemical reduction by cyclic voltammetry was measured by the method described in a previous report (9, 11).

Preparation of Primary Rat Hepatocytes

Primary rat hepatocytes were isolated from male specific pathogen-free Sprague-Dawley rats, weighing 200 to 250 g (8 to 10 weeks of age), and plated on a collagen substratum of 12 well plates with Dulbecco's Modified Eagle Media (Ginco Co. Ltd.) supplemented with fetal calf serum (5%), insulin (6.25 μg/mL), penicillin (50 μ/mL), streptomycin (50 μg/mL), and dexamethasone (1M) at a density of 3×10^3 viable

cells/dish. The cells were preincubated in the 5% CO_2 at 37°C for 20 h, exposed to chemicals for 24 h, and then cultured for a further 20 h in fresh medium. Cell viability was assessed by Trypan blue. The concentration of dimethylsulfoxide (DMSO) or distilled water was below 0.5% to avoid any cytotoxic influence. DNA was isolated from cells lysed with 2% sodium dodecyl sulfate at 37°C for 30 min. Portions of DNA materials were dissolved in a 10 mM sodium acetate buffer (pH 4.8) digested with 20 mg nuclease P1 at 37°C for 30 min, and then treated with 1.3 units of *Escherichia coli* alkaline phosphomonoesterase in 0.1M Tris-HCl buffer (pH 7.5) for 1 h.

Determination of 8-Oxoguanine (8-oxo-Gua)

Determination of 8-oxo-Gua was performed using the method reported previously (11, 13). After rat hepatocytes were stored at −80°C for 2 h, the materials were fused for 30 min in a CO_2 incubator and homogenized in a lysis solution with a Pozter-type homogenizer. The DNA was isolated from rat hepatocytes using a DNA extractor WB kit according to the method reported by Inoue et al. (12). All procedures were performed in a stream of nitrogen to prevent any artifacts during the DNA extraction. An authentic 8-oxo-Gua sample added to the cells consistently yielded in the range of 92% to 94%. The extracted DNA was dissolved in 100 μL of 1 mM EDTA and digested with 4 μL of nuclease P1 (5 mg/mL) and 2 L of acid phosphatase (47 mg/mL) suspension in 1.8 M $(NH_4)_2SO_4$ in the presence of 20 mM sodium acetate buffer at pH 4.5. After incubation at 37°C, the mixture was treated with 10 μL of ion exchange resin, Muromac (Muromachi Kagaku Kogyo, Tokyo, suspension, 50 mg/mL), and centrifuged at 15,000 × g for 5 min. The supernant was transferred to a filter tube (Millipore, Bedford, Massachusetts, USA; Samprep C; 0.2 μm) and centrifuged at 5,000 × g for 5 min. Then, the filtrate was injected into a high-pressure liquid chromatography column (HPLC). The 8-oxo-Gua concentration was determined using the HPLC-electrochemical detector (ECD) method, and the level was measured as the mean value repeated in triplicate two times.

RESULTS

Reduction Potential, LUMO Energy Levels, and Dihedral Angles of NPhs and NAPhs

Figure 1 illustrates the chemical structures of phenanthrene (Ph), 1-, 4-, 9-APhs, and 1-, 4-, and 9-APhOs. In this study, 22 NPhs and